Journal of Environmental Radioactivity 139 (2015) 140–148

Contents lists available at ScienceDirect

Journal of Environmental Radioactivity

journal homepage: www.elsevier.com/locate/jenvrad

Research note

Indoor terrestrial gamma dose rate mapping in France: a case study using two different geostatistical models

E. Warnery [a, b], G. Ielsch [a, *], C. Lajaunie [b], E. Cale [c], H. Wackernagel [b], C. Debayle [d], J. Guillevic [a]

[a] Institut de Radioprotection et de Sûreté Nucléaire, Bureau d'étude et d'expertise sur la radioactivité naturelle, IRSN, PRP-DGE, SEDRAN, BRN. BP17, 92262 Fontenay aux Roses, Cedex, France
[b] Mines ParisTech, Centre de Géosciences, Equipe de Géostatistique, 35 rue Saint Honoré, 77305 Fontainebleau, France
[c] Institut de Radioprotection et de Sûreté Nucléaire, Laboratoire de Dosimétrie de l'IRSN. IRSN/LDI. 31 rue de l'Ecluse, 78 294 Croissy Sur Seine Cedex, France
[d] Institut de Radioprotection et de Sûreté Nucléaire, Laboratoire de surveillance atmosphérique et d'alerte IRSN, PRP-ENV, SESURE, LS2A. BP 40035, 31 rue de l'écluse, 78116 Le Vésinet Cedex, France

ARTICLE INFO

Article history:
Received 6 May 2014
Received in revised form
7 October 2014
Accepted 8 October 2014
Available online 8 November 2014

Keywords:
Gamma dose rate
Uranium
Geology
Mapping
Geostatistics
France

ABSTRACT

Terrestrial gamma dose rates show important spatial variations in France. Previous studies resulted in maps of arithmetic means of indoor terrestrial gamma dose rates by "departement" (French district). However, numerous areas could not be characterized due to the lack of data. The aim of our work was to obtain more precise estimates of the spatial variability of indoor terrestrial gamma dose rates in France by using a more recent and complete data base and geostatistics. The study was based on the exploitation of 97 595 measurements results distributed in 17 404 locations covering all of France. Measurements were done by the Institute for Radioprotection and Nuclear Safety (IRSN) using RPL (Radio Photo Luminescent) dosimeters, exposed during several months between years 2011 and 2012 in French dentist surgeries and veterinary clinics. The data used came from dosimeters which were not exposed to anthropic sources. After removing the cosmic rays contribution in order to study only the telluric gamma radiation, it was decided to work with the arithmetic means of the time-series measurements, weighted by the time-exposure of the dosimeters, for each location. The values varied between 13 and 349 nSv/h, with an arithmetic mean of 76 nSv/h. The observed statistical distribution of the gamma dose rates was skewed to the right. Firstly, ordinary kriging was performed in order to predict the gamma dose rate on cells of 1*1 km^2, all over the domain. The second step of the study was to use an auxiliary variable in estimates. The IRSN achieved in 2010 a classification of the French geological formations, characterizing their uranium potential on the bases of geology and local measurement results of rocks uranium content. This information is georeferenced in a map at the scale 1:1 000 000. The geological uranium potential (GUP) was classified in 5 qualitative categories. As telluric gamma rays mostly come from the progenies of the ^{238}Uranium series present in rocks, this information, which is exhaustive throughout France, could help in estimating the telluric gamma dose rates. Such an approach is possible using multivariate geostatistics and cokriging. Multi-collocated cokriging has been performed on 1*1 km^2 cells over the domain. This model used gamma dose rate measurement results and GUP classes. Our results provide useful information on the variability of the natural terrestrial gamma radiation in France ('natural background') and exposure data for epidemiological studies and risk assessment from low dose chronic exposures.

Abbreviations: GUP, Geological uranium potential; TGDR, Indoor telluric gamma dose rates; LMC, Linear model of coregionalization; MCCK, Multi-collocated cokriging; OK, Ordinary kriging; WMM, Arithmetic mean of measurements at the same location, weighted by the time exposure of the dosimeters.

* Corresponding author. Tel.: +33 1 58 35 80 81; fax: +33 1 58 35 80 35.
E-mail addresses: eric.warnery@irsn.fr (E. Warnery), geraldine.ielsch@irsn.fr (G. Ielsch), Christian.Lajaunie@mines-paristech.fr (C. Lajaunie), eric.cale@irsn.fr (E. Cale), hans.wackernagel@mines-paristech.fr (H. Wackernagel), christophe.debayle@irsn.fr (C. Debayle), jerome.guillevic@irsn.fr (J. Guillevic).

http://dx.doi.org/10.1016/j.jenvrad.2014.10.002
0265-931X/

1. Introduction

Natural sources account for most of the population exposure to ionizing radiation. In particular, radon decay products and gamma rays emitted by terrestrial natural radionuclides found in the soil and in building materials contribute heavily to the dose. In France, natural sources that account for exposure to environmental radiation include radon (43%), terrestrial gamma rays (14%), cosmic rays (8%), and water and food (7%) (Rannou et al., 2006). The exposure is variable due to geographic location, housing characteristics, season, etc.

Terrestrial gamma radiation is emitted from naturally occurring radioisotopes, such as ^{40}K and the radionuclides from the ^{238}U and ^{232}Th series and their decay products. The levels of terrestrial gamma radiation are related to geology and uranium, thorium and potassium content of the rock from which the soils originate in each area. Indoor gamma dose rates may vary with geology, building materials, housing type and building period (Hatakka et al., 1998; Lyogi et al., 2002; Idrish Miah, 2001, 2004; Quindós Poncela et al., 2004, Rannou et al., 1984; Sundal and Strand, 2004; Szegvary et al., 2007).

In France, the study of Billon et al. (2005) allowed estimates of the French population's true exposure to natural ionizing radiation. The study provided a statistical description of the exposure and maps of arithmetic means of indoor radon concentrations, indoor and outdoor terrestrial gamma dose rates, and effective doses due to cosmic radiation, by “departement” (French district). The exposure indicators were corrected to reduce their variations due to several factors that influence measurements. In that study, 8737 indoor terrestrial gamma dose rate measurements yielded an average dose rate of 55 nSv/h (SD, 18 nSv/h), which ranged from 23 to 96 nSv/h over the 59 districts. There were also 5294 outdoor terrestrial gamma dose rate measurements with an average dose rate of 46 nSv/h (SD, 15 nSv/h), which ranged from 25 to 85 nSv/h over the 38 districts. These results provided useful exposure indicators of French population and allowed identifying areas with important variations. Nevertheless, numerous areas could not be characterized due to the lack of data (measurements available for only two-thirds of the country) and precise estimation of the spatial variability of indoor terrestrial gamma dose rates could not be obtained.

The spatial interpolation methods, including geostatistics, have been developed for and applied to various disciplines. Ordinary kriging and cokriging are two geostatistical techniques used to create continuous maps of spatially autocorrelated attributes. These techniques have been commonly used in environmental sciences, soils sciences, medical/health sciences and have been sometimes compared for spatial interpolation of data (Carter et al., 2011; Goovaerts, 1999, 2011; Knotters et al., 1995; Liu et al., 2006; Moral, 2010; Oliver et al., 1998). These geostatistical techniques can also be applied to map natural or artificial radioactivity (Baume et al., 2011; Buttafuoco et al., 2010; Caro et al., 2013; Dubois et al., 2007; Guagliardi et al., 2013; Guastaldi et al., 2013; Mabit and Bernard, 2007; O'Dea and Dowdall, 1999; Sanusi et al., 2014; Szegvary et al., 2007). Ordinary kriging (Sanusi et al., 2014; Szegvary et al., 2007) and more rarely cokriging (Guastaldi et al., 2013) have been used in recent studies for interpolating gamma radiation levels.

The aim of our work was to obtain better indicators of the spatial variability of indoor terrestrial gamma dose rates in France by using more recent and complete data, and geostatistics. The study was based on 97,595 measurement results distributed in 17,404 locations covering the whole French territory. Measurements were done by the Institute for Radioprotection and Nuclear Safety (IRSN) using RPL (Radio Photo Luminescent) passive dosimeters, exposed during several months between 2011 and 2012, in French dental surgeries and veterinary clinics. The results used came from dosimeters which were not exposed to anthropic sources. Moreover, the IRSN developed in 2010 a map of the uranium potential of French geological formations, on the basis of geology and local measurement results of rocks uranium content. The geological uranium potential (GUP) was classified in 5 qualitative categories. As telluric gamma rays mostly come from the progenies of the ^{238}U series present in rocks, this information, which is exhaustive throughout France, has also been used for estimating the telluric gamma dose rates.

2. Materials and methods

2.1. Data source: results of indoor gamma dose rate measurements

For this study, data has been provided by the LDI (Laboratoire de Dosimétrie de l'IRSN). The data were collected between 2011 and 2012, as part of the routine monitoring of French dentist surgeries and veterinary clinics. The dosimeters were not exposed to anthropic radioactive sources and thus reflect the background of the gamma radiations in buildings. The dosimeters were the RPL technology (Radio Photo Luminescent) where RPL refers to the luminescence arising through interaction with ionizing radiation and induced to emission by the action of ultraviolet light. The detector is a silver-doped glass of phosphate. The luminescent properties of the glass derived from a very small concentration of doping agents (silver ions) where Ag + acts as traps for both electrons and positive holes. These traps are metastable, so that stimulation with ultraviolet light causes the electrons in the traps to move to an energy level above their state and to return to it with the release of luminescence in visible range. The intensity of this luminescence is directly proportional to the dose received. A combined system of 5 different filters allows to compare doses from beta, X and gamma radiation. The principal advantage comes from the fact that since the traps are metastable, the signal is not erased by the read-out procedure but remains indefinitely, allowing the measurement to be reproduced. It has very low fading and low sensitivity to the environmental temperature. Nanto et al. (2011) and Ranogajec-Komor et al. (2008) indicate that RPL dosimeters, commonly used for personal monitoring, are also suitable for monitoring environmental and ambient radiation. After reading and processing with a special algorithm, measurements count the absorbed dose of gamma radiation received during the total time exposure of the detector with an accuracy of 20%.

LDI data are usually related to monthly and quarterly measurements which correspond to the workers chronological follow-up. In order to harmonize those measurements and study a gamma dose rate, all the data have been divided by the corresponding time exposure which lies between 20 and 180 days. The data base counts 98 858 measurements distributed at 17 420 locations in France (Fig. 1). The density of measurement sites is variable, with clusters of measurements in the biggest cities. Areas where few measurements are available correspond to the areas with the lowest population density. All locations do not have the same number of measurements (the number varies between 1 and 29). More than 90% of the data is constituted of quarterly measurements and on average there are 6 measurement results per location.

2.2. Auxiliary information: uranium potential of geological formations

The IRSN achieved in 2010 a classification of French geological formations, characterizing a uranium potential on the bases of several criteria such as geology and local means of uranium content

(Ielsch et al., 2010). This information is georeferenced in vectored polygons of a 1:1 000 000 geological map. The geological uranium potential (GUP) has been classified into 5 qualitative categories from 1 for the rocks containing less uranium up to 5. As telluric gamma radiations mostly stems from the progenies of the ^{238}U series present in rocks, this type of information, which is exhaustively known for the whole of France, could provide a basis for estimating telluric gamma dose rates.

2.3. Calculating natural terrestrial gamma dose rate

Measurements merge the different contributions of terrestrial and cosmic gamma dose rates. The self-effect which is the response of the dosimeter in a zero-radiation environment, has not been taken into account. Indeed, its value can be considered negligible compared to the accuracy of the dosimeter. The artificial radiation contribution, which directly comes from the presence of ^{137}Cs in soils after nuclear weapon tests and nuclear power plant accidents, was also considered negligible. At ground level, the cosmic radiation is mainly coming from muons. According to the UNSCEAR report (2008), exposure to cosmic rays is strongly dependent on altitude while variation with latitude is small, about 10% between equator and high latitudes.

Estimation of cosmic gamma dose rates at the different measurement locations were calculated using the formulas published in the UNSCEAR Report (2008) from Bouville and Lowder (1988):

$$E_1(z) = E_1(0).\left[0.21e^{-1.649z} + 0.79e^{0.4528z}\right] \ \left(\mu Sv/y\right),$$

with the mean dose rate at sea level, $E_1(0)$ equals to 240 μSv/y and z, the altitude in km.

Those estimates have then been subtracted from the RPL measured values in order to keep the natural terrestrial part of the gamma radiations.

2.4. Outliers removal

Outlying values which do not reflect the global trend of the other measurements were identified at various locations. In a first approach, the highest values exceeding the threshold of 300 nSv/h were studied carefully. Comparisons between the measured values at a given location and at neighboring locations were done. The effects of local statistics (in a spatial neighborhood) and geology were also taken into account. Finally 19 values at 9 sites were removed. In order to take care of other inconsistencies, a filter was designed. All differences between measurements of the same location were computed; when two data differed from each other by more than 50 nSv/h, the sample value farthest from the median was removed. This procedure led to the exclusion of about 1% of the total number of measured values and it removed completely 15 locations.

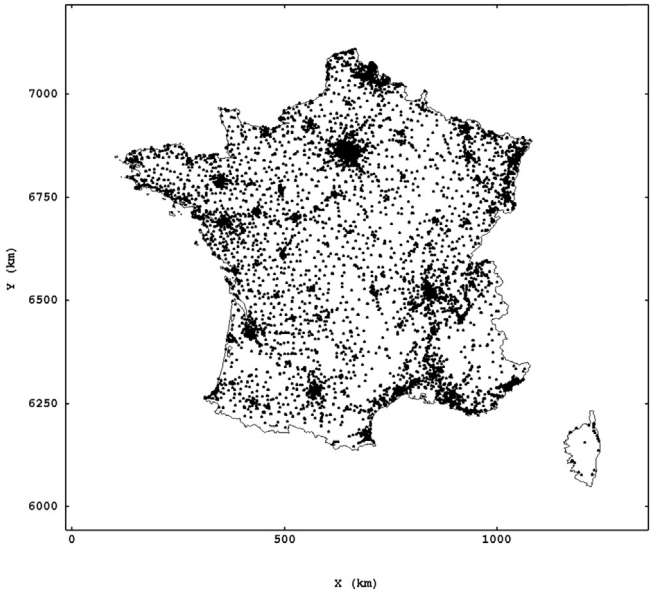

Fig. 1. Distribution of the 17 420 measurements locations over French territory.

2.5. Time variations of indoor gamma dose rate measurements

The data base provides different measurements for each location during the period 2011–2012. Fluctuations were observed in time-series without particular trend, which might be due to low seasonal variations of the gamma dose rates, varying time-exposure of the dosimeters or dosimeter precision. As the number of measurements per location differed, it appeared necessary to find a relevant process for estimating a single and representative value of the gamma dose rate for each location. A mathematical model was built considering each measured value as a combination of two terms: one spatial component (free of time-variation and depending only on the location) and a random time-varying component (assumed to be spatially and temporally uncorrelated). This model allowed estimating the experimental variogram of the constant-in-time component of the measurements, avoiding the support-effect (due to the differences of the dosimeters' time-exposure) and taking into account the intrinsic variability of each time-series. Results showed that the shape of this particular variogram was very similar to the one computed experimentally with the arithmetic means of measurements weighted by the time-exposure of the dosimeters (WMM). Finally this model showed that differences of support and time-series fluctuations were negligible with regard to spatial variability. Thus the WMM was considered as a single and representative value of the gamma dose rate at each location.

2.6. Spatial distribution of data and declustering

The spatial density of measurements was not constant over the domain. More than 50% of the data were clustered in few areas and the largest clusters corresponded to the major cities of the country (Fig. 1). A declustering procedure was needed to reduce the influence of densely sampled areas. A moving window approach was thus designed to weigh each observation relatively to the number of available samples. The size of this moving window was calibrated considering the average distance between samples, which was between 10 and 25 km. After several tests, a moving window size of 10*10 km^2 was retained.

2.7. Geostatistical analysis

2.7.1. Ordinary kriging

Ordinary Kriging (OK) is the estimator used in geostatistics for estimating values at unsampled locations and is one of the most frequently used functions for mapping environmental data. The term “regionalized variable” is used to designate a numerical function $z(x)$ that is dependent on the spatial location x. In order to quantify and model the spatial variability, geostatistics use specific tools such as the experimental variogram. Several types of mathematical models allow fitting the corresponding experimental function. A variogram model can then be fitted through the choice

of different parameters such as the nugget effect, the sill and the range. Once a variogram model has been chosen, the kriging system allows predicting values at unsampled locations. The interpolation of an unknown value $Z(x_0)$ at point x_0 is seen as a linear combination of the nearby measurements $Z(x_i)$:

$$Z(x_0) = \sum_{i=1}^{N} \lambda_i . Z(x_i)$$

The weights λ_i of the linear combination depend on the distance $|x_i - x_0|$ and the degree of variability expressed by the variogram model.

OK represents the Best Linear Unbiased Estimator (BLUE), as it ensures a zero mean for the estimation error and it minimizes the estimations variance ($\mathrm{Var}(z^*(x_0) - z(x_0))$). We refer the reader to the standard literature in the field; see, e.g.; Chilès and Delfiner (2012) for details.

2.7.2. Multi-collocated cokriging

Multivariate geostatistics is used to take advantage of structural relations between variables. These relations can be used to improve the estimation of one variable by introducing data from others. A multivariate structural model, such as the linear model of coregionalization (LMC) is needed to this aim. After modeling, the cokriging system, taking the example of only one additional variable Z_2, allows using data of both variables Z_1 and Z_2 for predicting values at unsampled locations of Z_1. The prediction of Z_1 at point x_0 is performed with a linear combination of the nearby measurements of $Z_1(x_i)$ and $Z_2(x_i)$:

$$Z_1^*(x_0) = \sum_{S1} \lambda_{1i} Z_1(x_i) + \sum_{S2} \lambda_{2i} Z_2(x_i)$$

The weights λ_{1i} and λ_{2i} depend on the distance $|x_i - x_0|$ and the structure of the variogram and cross-variogram model. S_1 and S_2 are the two sets of locations where the variables Z_1 and Z_2 are respectively known.

The improvement obtained over the ordinary kriging is substantial if the correlation between the two variables is high, and if the auxiliary variable is densely sampled. The cokriging system can then become large, and simplifications are useful. The most common simplifications were reviewed in Rivoirard (2004). In the multi-collocated cokriging the auxiliary variable is used only where the target variable is available and at the current point to be estimated. This special procedure is usually an approximation of the original cokriging commonly used. However, it has been shown in Rivoirard (2001) that this procedure is exact when joint structure of the two variables is such that the cross-covariance is proportional to the covariance of the auxiliary variable.

3. Results

3.1. Exploratory data analysis

3.1.1. Global statistics of indoor telluric gamma dose rates

Considering the WMM, the number of indoor telluric gamma dose rates (TGDR) observations was 17 404, corresponding to the number of measurement sites, after the outliers removal. The observed statistical distribution of the data was skewed to the right (Fig. 2). The levels varied between 13 and 349 nSv/h, with a mean of 76 nSv/h and a median of 70 nSv/h. The bulk of the values varied between 20 and 120 nSv/h. The relative standard deviation (RSD) was equal to 0.44, showing that the values were moderately scattered around the mean.

An arithmetic mean of TGDR was calculated for each "departement" (administrative unit in France), considering the WMM obtained at each location (Fig. 3). These values lay between 39 and 155 nSv/h. Higher gamma dose rates were generally observed in areas characterized by Hercynian granitic rocks, such as in the "Massif Armoricain", the "Massif Central" and in Corsica.

3.1.2. Global statistics considering the geological uranium potential

The auxiliary variable, the geological uranium potential (GUP) is categorical and represents qualitative information. Therefore, in order to compare it with TGDR and to use it in cokriging, it was necessary to transform it as a quantitative variable. As it is usually done in this case (Jeannée and De Fouquet, 2003), the means of the TGDR per classes of GUP were considered. The global statistics of indoor gamma dose rates per class of GUP (Table 1, Fig. 4) showed that these gamma dose rates were quite scattered in each class, nevertheless the mean, the median and the frequency of higher values increased accordingly to the GUP until class {4}. The statistics observed for class {5} were quite similar to that of class {4}. This could be related to the low number of data available for this class.

3.2. Modeling and kriging

3.2.1. Ordinary kriging of indoor telluric gamma dose rates

The experimental variogram considered for the study was obtained by declustering the data with a moving cell of 10*10 km^2. Considering the width of the domain studied and the high number of samples available, the variogram model has been fitted up to a lag of 125 km. Indeed considering a circular area of 100 km radius, at least 100 neighbor samples were available, everywhere in the domain, even in the areas with the lowest sampling density. The experimental variogram did not vary with direction which led to choosing an isotropic variogram model. Comparison of different models was done by leave-one-out cross validation. The prediction efficiency of different models was compared statistically, over the whole domain and through different selections, on the basis of the error and the standardized error of data re-estimation. The best results led to a nested variogram model of 3 spherical structures

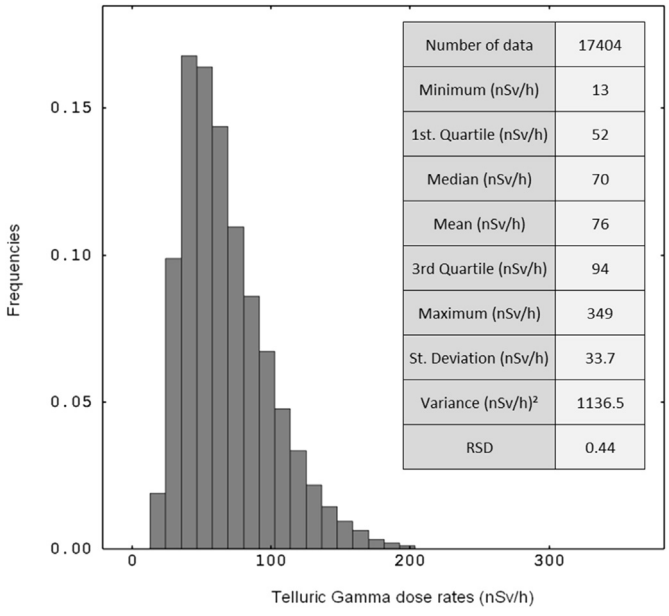

Fig. 2. Histogram of the WMM (arithmetic gamma dose rate means weighted by the dosimeters' time-exposure) and global statistics. RSD: relative standard deviation.

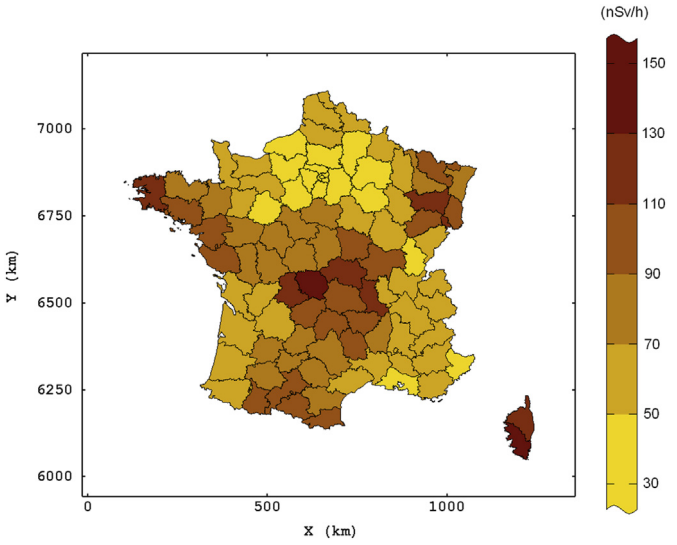

Fig. 3. Arithmetic mean of the indoor telluric gamma dose rates for each "departement" (administrative unit in France).

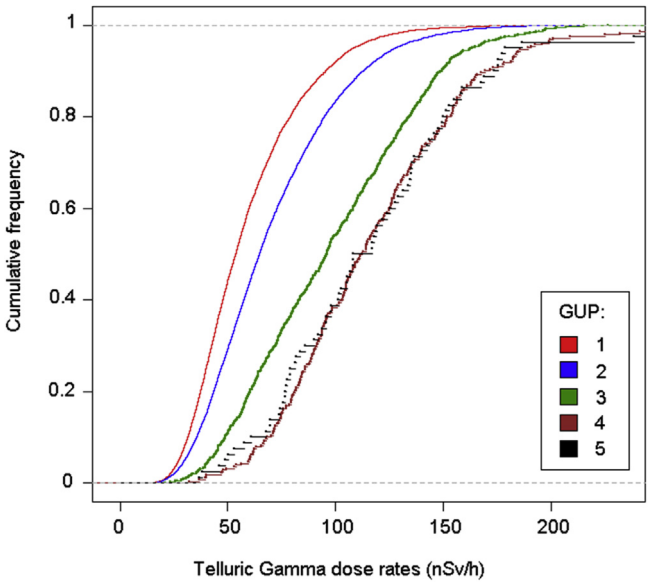

Fig. 4. Distribution of the telluric gamma dose rates per classes of geological uranium potential (GUP).

with a nugget effect of 310 $(nSv/h)^2$ and a total sill of 879 $(nSv/h)^2$ (Fig. 5). The ratio of nugget effect over total sill variance was about 35%, which indicated that the TGDR had a modest spatial continuity.

OK was performed in order to predict an averaged gamma dose rate on cells of 1*1 km^2, all over the domain. The neighborhood used for the estimation was a circular area of 100 km radius, divided into 4 sectors (20 nearest samples for each one). The optimal number of samples used was 80. The prediction map obtained (Fig. 6) showed that the range of the values varied from 28 to 230 nSv/h. This range was more restricted than the measured data, as a consequence of the smoothing properties of kriging. The standard deviation of the kriging error was clearly driven by the samples density. The lowest value (about 2 nSv/h), was reached in the most clustered areas and the highest (20 nSv/h) occurred in the largest gaps of data.

3.2.2. *Multi-collocated cokriging: using auxiliary information*

Cokriging methods allow using an auxiliary variable linked to the one of interest. The information brought by the GUP was used as an auxiliary variable in MCCK models. Depending on the correlation between both variables and also on data configuration, the estimation of TGDR could benefit from this secondary information. The best correlation between gamma dose rates and their mean per class of GUP was obtained through the declustered data. It also turned out that grouping classes {4} and {5} had no influence on the correlation coefficient which was equal to 0.44. Moreover, a small number of samples was available in each of the classes. Therefore, classes {4 + 5} were grouped into a unique category.

In case of cokriging two variables, the experimental model to be fitted is composed of two simple variograms and one cross-variogram (Fig. 7). As in the previous estimation by OK, isotropic models were fitted using empirical estimate at distances up to 125 km. Through different cross validation results, a nested model combining a nugget effect and spherical structures was chosen (Table 2). The previous model chosen for the TGDR in OK prediction was preserved at best. Multi-collocated cokriging (MCCK) was performed on 1*1 km^2 cells, over the whole domain, using the same neighborhood as for OK. Estimated values varied from 28 to 229 nSv/h (Fig. 8). The standard deviation of the estimation error was dependent on the sampling density as for OK model. The standard deviation of MCCK is necessarily lower or equal to the OK standard deviation.

4. Discussion

4.1. *Ordinary kriging and multi-collocated cokriging comparison*

4.1.1. *Behavior of estimation maps and comparison of results*

The comparison between the prediction maps obtained with OK or MCCK present similar results (Figs. 6 and 8). The regions characterized by the highest gamma dose rates (from 120 to 230 nSv/h) are well known to be generally granitic or metamorphic areas: "Massif Armoricain" in the North-West, "Vosges" in the North-East, "Massif Central" in the center, "Pyrenees" in South-West and Corsica. The lowest values (from 28 to 50 nSv/h) are observed in the "Bassin Parisien", in North of France and along the Rhône Valley which goes down until the Mediterranean coast. As both estimation maps are quite similar, their prediction efficiency has been evaluated through cross-validation. The comparison criterion selected

Table 1
Global statistics of indoor telluric gamma dose rates per class of GUP.

GUP	Number of data	Rank mean	Mean (nSv/h)	Median (nSv/h)	Variance $(nSv/h)^2$	Minimum (nSv/h)	Maximum (nSv/h)
{1}	7244	7299	66	61	682	13	218
{2}	8826	9180	77	72	897	13	227
{3}	975	12 683	105	99	1451	21	288
{4}	279	14 543	129	123	2731	32	349
{5}	80	14 260	123	117	1874	37	264
{4 + 5}	359	14 480	128	121	2555	32	349

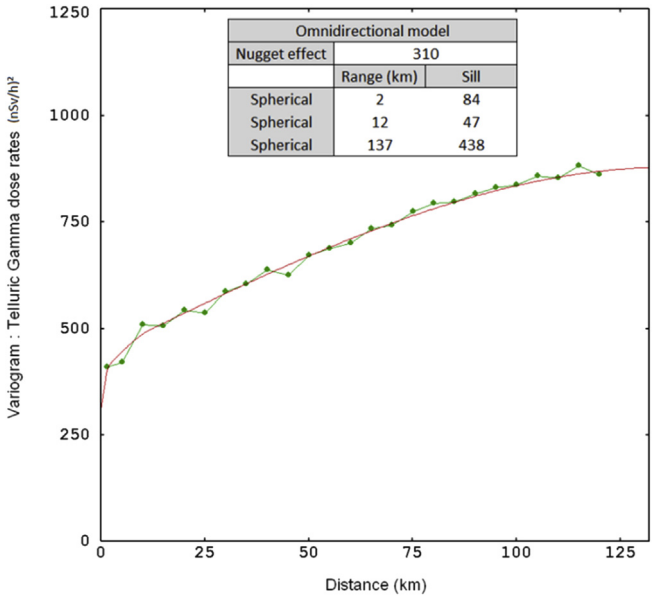

Fig. 5. Omnidirectional variogram of indoor telluric gamma dose rates; model fitted for OK and parameters of the model.

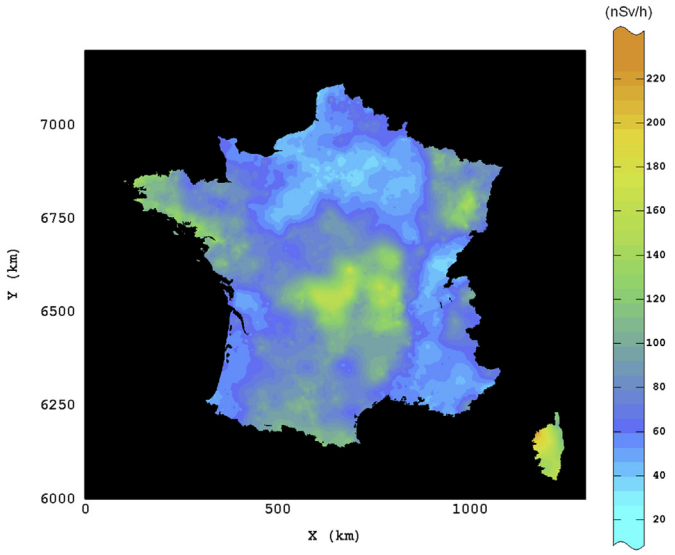

Fig. 6. Estimation map of the indoor telluric gamma dose rates over French country, from OK.

was the mean square error (MSE[1]) which measures the average squared difference between the true values $Z(x)$ and the predicted ones $Z^*(x)$. Although the difference between models was really low, about 0.5%, the different results of MSE allowed appreciating the improvements of MCCK (Table 3). Moreover, considering a 10*10 km^2 moving-cell declustering process, the MCCK allowed decreasing 2.2% of MSE, relatively to the OK. This last declustering allowed reducing the influence of clusters in the cross validation results, i.e. it allowed spatially averaging errors, avoiding the weight introduced by the irregular density of samples among the domain. The re-estimation of known data has been done over a spatial regular selection of samples taken from the initial data base. This selection named GS_10 has been made by taking randomly one unique sample per cell of 10*10 km^2 among the domain, avoiding thus any cluster of data. Re-estimating such a spatially-regular selection, on the basis of the whole known data base, allowed appreciating the MSE's relative improvement of MCCK over OK, which was about 2.1% (Table 3). Finally those results showed that globally over the domain, MCCK is generally more efficient than OK.

4.1.2. Comparison through random selections

The information brought by the GUP could be hidden by the high number of samples initially contained in the data base. Therefore, it was tested to re-estimate different selections by cross validation, reducing the number of known data. The cross validation was performed, re-estimating different GS_10 selections of samples. Those selections were made, as previously, taking randomly one unique sample per cell of 10 × 10 km^2 within the domain, avoiding clusters. In order to reduce fictitiously the number of known data for the re-estimation, different selections named S_25% were created. Those S_25% selections, used to represent different cases of sparsely sampled domains, were 25% of randomly selected samples within the initial data base. The results obtained showed that the relative MSE improvement of MCCK over OK varied from 1.6 to 5% (Table 3).

[1] $\mathrm{MSE} = 1/N\sum_{i=1}^{N}[Z(x) - Z^*(x)]^2$. Where N is the number of samples selected in the cross-validation process.

4.1.3. Regional analysis

The maps of both estimations (Figs. 6 and 8) were compared at a regional scale. Some differences could be visually observed: for example the map from MCCK was more detailed in some areas, stamped by the map of GUP (Fig. 9). Comparisons of the regional MSE was also done, with cross validation of the whole data base. For 16 administrative regions over a total of 22, the relative differences between OK and MCCK were lower than 1% and considered as non-relevant. For 6 regions, the results showed a difference above 1% (Table 4). For four regions the MCCK allowed improving the estimation. Furthermore, the MCCK improved the MSE of most of the regions concerned by moderate-to-high gamma dose rates. One exception is Corsica: the different behavior stems from the fact that geographically Corsica is quite away from the rest of France and that the global modeling could then be less representative for this region; moreover few measurements are available for the island. However, the results showed that globally the MCCK model gave a better estimation and allowed designing more realistic outlines in the estimation map.

4.1.4. Comparison through the geological uranium potential classes

The difference of estimation $Z^{OK} - Z^{MCCK}$ was calculated for the different GUP classes. The results showed that the mean of the difference was increasing with GUP classes. Considering GUP classes {1} and {2}, the difference was quite low and well balanced around zero. For the GUP classes {3} and {4 + 5}, the estimation obtained by MCCK was higher than the one obtained by OK. A cross-validation process was performed for both models with respect to each class of GUP. For the class {4 + 5}, MCCK allowed improving the MSE by 4.3% relatively to the OK (Table 5). In the other classes, an improvement by MCCK was also observed, in spite of really low gain. Those results seem to confirm what had been observed with the regional analysis: the MCCK model provided a better estimation than the OK model in areas with high gamma dose rates.

4.2. Contribution of the study

This study yields new results on French population exposure to indoor terrestrial gamma rays, based on a recent and more complete data base than in earlier studies (Billon et al., 2005; Szegvary

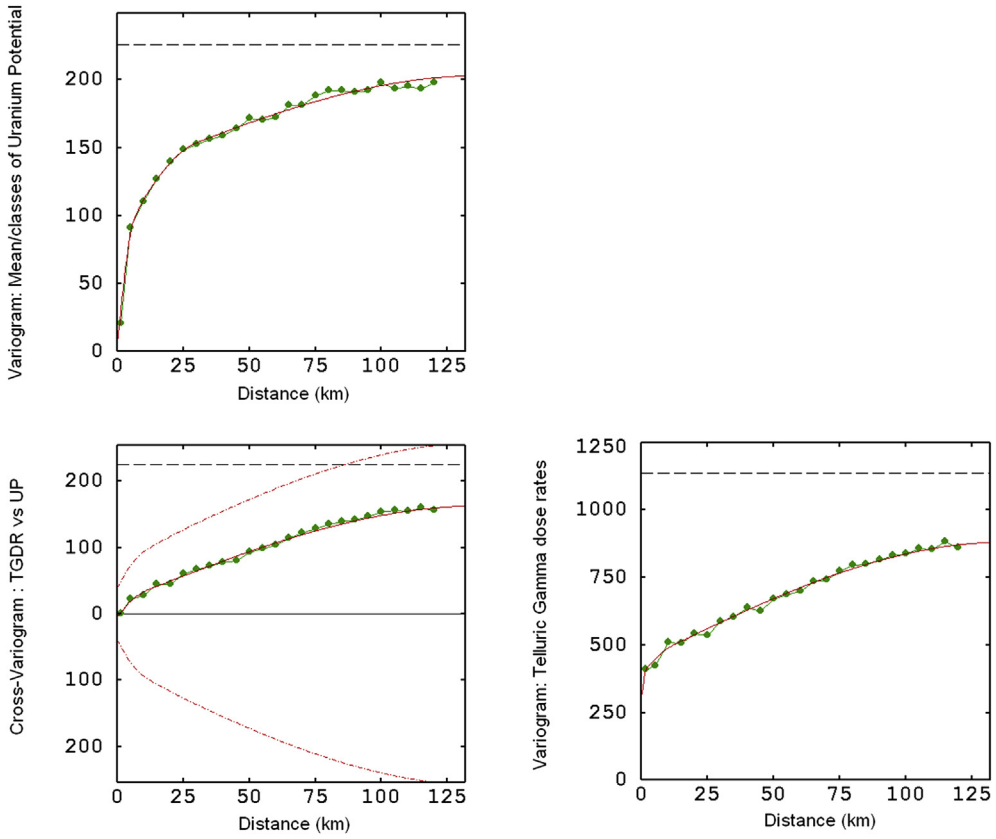

Fig. 7. Omnidirectional variograms and cross variogram for the indoor telluric gamma dose rates (TGDR) and the mean per classes of geological uranium potential (UP).

et al., 2007). When compared to earlier results, some differences can be observed: the range of TGDR reaches higher values (13 and 349 nSv/h) and the mean (76 nSv/h) is higher. Moreover, the comparison of the maps of the mean TGDR for each "departement" (French district) obtained in the present study and by Billon et al. (2005) shows similar global spatial variations with, nevertheless, some differences: our results exhibit higher means for some "departements" (values globally ranging between 39 and 155 nSv/h) and furthermore the whole territory could be covered. The study of Billon et al. (2005), based on 8737 results, shows an average dose rate of 55 nSv/h, with measurements ranging from 23 to 96 nSv/h over 59 "departements".

Compared to statistical analysis, estimates realized by geostatistical methods have brought more precise indicators of the spatial variability of TGDR. The maps allow highlighting different "hot spots", avoiding unrealistic descriptions at subdivision borders such as administrative units. The intrinsic variability of the phenomenon can be appreciated through the whole domain and moderate to high variations at low distances can be observed. Nevertheless, the models, as all kriging models, tend to smooth the data as prediction maps obtained in the present study showed values varying between 28 and 230 nSv/h, while measured levels range between 13 and 349 nSv/h.

Geostatistical analysis was used in a previous study (Szegvary et al., 2007) to realize European maps of terrestrial gamma dose rate based on routine monitoring data. For France, outdoor measurement results from a network of 168 stations were used. The results showed levels ranging between 0 and 180 nSv/h for Europe. Our results are globally consistent with the main "hot spots" observed in the "Massif Central" and "Bretagne" on these European maps. Considering the differences of mapping scale and of data base used for France, our results allow estimating with more accuracy spatial variations of terrestrial gamma dose rates. The higher levels observed in the present study can be explained by differences in the network density, the location of measurements (indoor of outdoor) and the type of dosimeters used.

5. Conclusions

The aim of our work was to obtain more precise estimates and maps of the spatial variability of indoor terrestrial gamma dose rates in France by using two recent and more complete data

Table 2
Parameters used in the multilinear model adjusted through the Linear model of coregionalization constraints.

Variograms	Nugget effect	Spherical range (km) 2	Spherical range (km) 6.5	Spherical range (km) 12	Spherical range (km) 30	Spherical range (km) 137
	Sill	Sill	Sill	Sill	Sill	Sill
Telluric gamma dose rates	310	84	1	47	1	438
Mean/classes of GUP	5	0	63	13	49	73
Cross variogram	−5	0	7	16	0	145

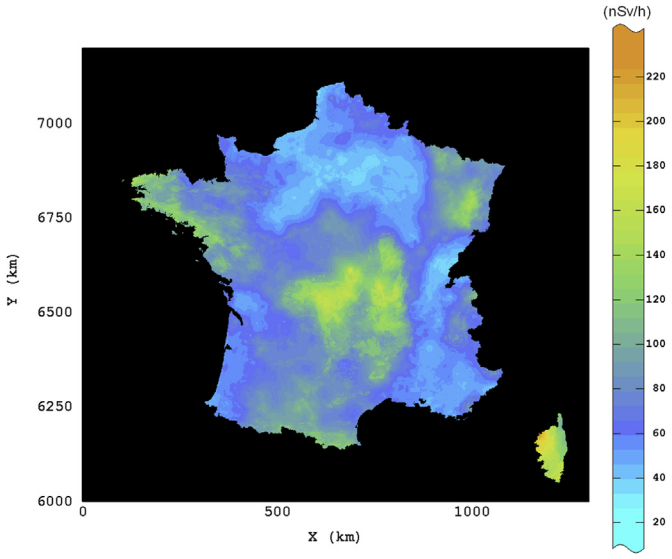

Fig. 8. Estimation map of the indoor telluric gamma dose rates over French country, from MCCK.

bases and geostatistics. The study was based on 97 595 measurements results at 17404 locations covering the whole of France and a map of geological uranium potential. Two geostatistical methods were compared to obtain the best estimation. Ordinary kriging used the initial data base of measurements while multi colocated co-kriging offered the possibility to combine a secondary variable, the geological uranium potential, known exhaustively over the domain. The models were applied to predict the average indoor telluric gamma dose rate on cells of 1*1 km^2.

The measurement results of TGDR showed that the arithmetic mean of measurements at the same location, weighted by the dosimeters time exposure, varied between 13 and 349 nSv/h, with a mean of 76 nSv/h and a median of 70 nSv/h. An arithmetic mean of the gamma dose rates was calculated for each "departement" (administrative unit in France), and these mean values ranged between 39 and 155 nSv/h. Higher gamma dose rates were generally observed in areas where Hercynian granitic rocks are observed, such as in western ("Massif Armoricain"), in the central ("Massif Central") France and in Corsica.

The means of TGDR per class of geological uranium potential were considered for the multi colocated co-kriging model. The gamma dose rates distributions in each class of geological uranium potential showed that the mean of each category increased accordingly to the GUP class.

Estimation models (OK and MCCK) provided relatively similar results. The prediction maps obtained showed that the range of the values varied from 28 to 230 nSv/h. The results allowed appreciating the improvements of MCCK, particularly by comparing estimates at a regional scale. This model gave a better estimation for most of the regions concerned by moderate-to-high gamma dose rates.

The present work provides new results on the French population exposure to indoor terrestrial gamma rays, based on two recent and more complete data bases. The estimates realized by geostatistical methods bring more precise indicators of the spatial variability of TGDR.

Table 3
Comparison of MSE's results from different cross-validations using different selections of data.*: the statistical results used a declustering process within a moving cell of 10 × 10 km^2.

Re-estimated data		Selection of known values for the estimation		MSE (nSv/h)^2		Relative improvement of MCCK
Selection	Number of measurements	Selection	Number of measurements	OK	MCCK	
ALL	17404	ALL	17404	409	407	0.5%
ALL*	17404	ALL*	17404	510	499	2.2%
GS_10-1	2743	ALL	17404	483	473	2.1%
GS_10-3	2739	S_25%-1	4248	441	419	5.0%
GS_10-4	2739	S_25%-2	4407	387	381	1.6%
GS_10-5	2733	S_25%-3	4382	373	362	2.9%

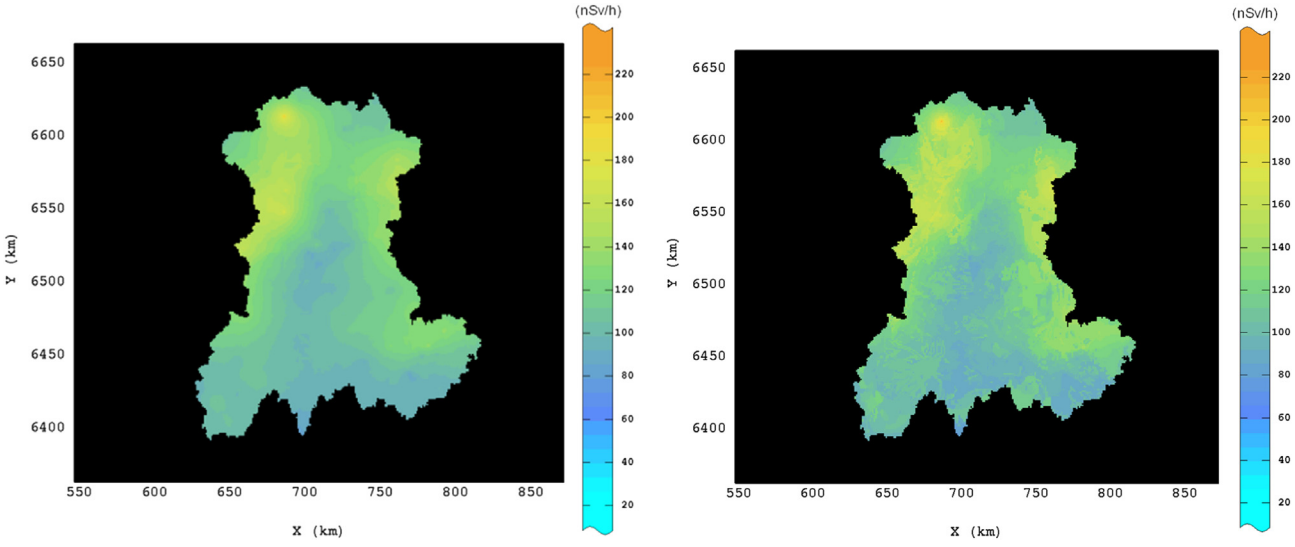

Fig. 9. Estimation differences at regional scale: example of the region 'Auvergne', with the OK estimation (left) versus the MCCK estimation (right).

Table 4
Comparison of MSE's results from regional cross-validations.

Re-estimated data		Selection of known values for the estimation		MSE $(nSv/h)^2$		Relative improvement of MCCK
Selection	Number of measurements	Selection	Number of measurements	OK	MCCK	
Auvergne	305	ALL	17404	853.1	833.0	2.4%
Bourgogne	434	ALL	17404	527.9	520.2	1.5%
Bretagne	1019	ALL	17404	577.5	563.9	2.4%
Limousin	206	ALL	17404	702.0	692.3	1.4%
Basse Normandie	321	ALL	17404	317.6	321.9	−1.4%
Corse	63	ALL	17404	1266.0	1296.4	−2.4%

Table 5
Comparison of MSE's results from cross-validations considering the GUP classes.

Re-estimated data		Selection of known values for the estimation		MSE $(nSv/h)^2$		Relative improvement of MCCK
GUP	Number of measurements	Selection	Number of measurements	OK	MCCK	
{1}	7244	ALL	17404	318	318	0.0%
{2}	8826	ALL	17404	399	398	0.3%
{3}	975	ALL	17404	796	795	0.1%
{4 + 5}	359	ALL	17404	1451	1389	4.3%

These results could provide useful guidance for the identification of areas with high levels of natural radiation and radon, for the evaluation of the natural radiation background, for the estimation of the exposure to natural ionizing radiation, or for epidemiological studies and risk assessment from low dose chronic exposures.

References

Baume, O., Skøien, J.O., Heuvelink, G.B.M., Pebesma, E.J., Melles, S.J., 2011. A geostatistical approach to data harmonization – application to radioactivity exposure data. Int. J. Appl. Earth Observ. Geoinf. 13, 409–419.

Billon, S., Morin, A., Caer, S., Baysson, H., Gambard, J.P., Backe, J.C., Rannou, A., Tirmarche, M., Laurier, D., 2005. French population exposure to radon, terrestrial gamma and cosmic rays. Radiat. Prot. Dosim. 113 (3), 314–320.

Bouville, A., Lowder, W.M., 1988. Human population exposure to cosmic radiation. Radiat. Prot. Dosim. 24, 293–299.

Buttafuoco, G., Tallarico, A., Falcone, G., Guagliardi, I., 2010. A geostatistical approach for mapping and uncertainty assessment of geogenic radon gas in an area of southern Italy. Environ. Earth Sci. 61, 491–505.

Caro, A., Legarda, F., Romero, L., Herranz, M., Barrera, M., Valiño, F., Idoeta, R., Olondo, C., 2013. Map on predicted deposition of Cs-137 in Spanish soils from geostatistical analyses. J. Environ. Radioact. 115, 53–59.

Carter, G.P., Miskewitz, R.J., Isukapalli, S., Mun, Y., Vyas, V., Yoon, S., Georgeopoulos, P., Uchrin, C.G., 2011. Comparison of kriging and cokriging for the geostatistical estimation of specific capacity in the Newark Basin (NJ) aquifer system. J. Environ. Sci. Health A Tox Hazard Subst. Environ. Eng. 46 (4), 371–377.

Chilès, J.P., Delfiner, P., 2012. Geostatistics. Modeling spatial uncertainty. In: Wiley Series in Probability and Statistics, second ed. John Wiley & Sons. 699 pp.

Dubois, G., Bossew, P., Friedmann, H., 2007. A geostatistical autopsy of the Austrian indoor radon survey (1992-2002), 15 Sci. Total Environ. 377 (2–3), 378–395.

Goovaerts, P., 1999. Geostatistics in soil science: state-of-the-art and perspectives. Geoderma 89, 1–45.

Goovaerts, P., 2011. A coherent geostatistical approach for combining choropleth map and field data in the spatial interpolation of soil properties. Eur. J. Soil Sci. 62, 371–380.

Guagliardi, I., Buttafuoco, G., Apollaro, C., Bloise, A., De Rosa, R., Cicchella, D., 2013. Using gamma-ray spectrometry and geostatistics for assessing geochemical behaviour of radioactive elements in the Lese Catchment (southern Italy). Int. J. Environ. Res. 7 (3), 645–658, 2013.

Guastaldi, E., Baldoncini, M., Bezzon, G., Broggini, C., Buso, G., Caciolli, A., Carmignani, L., Callegari, I., Colonna, T., Dule, K., Fiorentini, G., Kaçeli Xhixha, M., Mantovani, F., Massa, G., Menegazzo, R., Mou, L., Rossi Alvarez, C., Strati, V., Xhixha, G., Zanon, A., 2013. A multivariate spatial interpolation of airborne γ-ray data using the geological constraints. Remote Sens. Environ. 137, 1–11.

Hatakka, J., Paatero, J., Viisanen, Y., Mattson, R., 1998. Variations of external radiation due to meteorological and hydrological factors in central Finland. Radiochemistry 40 (6), 534–538.

Idrish Miah, M., 2001. Study on the variation of indoor gamma radiation in the Dhaka district. Radiat. Prot. Dosim. 95, 365–370.

Idrish Miah, M., 2004. Environmental gamma radiation measurements in Bangladeshi houses. Radiat. Meas. 38, 277–280.

Ielsch, G., Cushing, M.E., Combes, Ph, Cuney, M., 2010. Mapping of the geogenic radon potential management: methodology and first application. J. Environ. Radioact. 101, 813–820.

Jeannée, N., De Fouquet, C., 2003. Apport d'informations qualitatives pour l'estimation des teneurs en milieux hétérogènes : cas d'une pollution des sols par des hydrocarbures aromatiques polycicliques (HAP). Comptes Rendus Géosci. 335 (5), 441–449.

Knotters, M., Brus, D.J., Oude Voshaar, J.H., 1995. A comparison of kriging, co-kriging and kriging combined with regression for spatial interpolation of horizon depth with censored observations. Geoderma 67, 227–246.

Liu, T.L., Juang, K.W., Lee, D.Y., 2006. Interpolating soil properties using kriging combined with categorical information of soil maps. Soil Sci. Soc. Am. J. 70, 1200–1209.

Lyogi, T., Ueda, S., Hisamatsu, S., Kondo, K., Haruta, H., Katagiri, H., Kurabayashi, M., Nakamura, Y., Tsuji, N., 2002. Environmental gamma-ray dose rate in Aomori Prefecture. Jpn. Health Phys. 82, 521–526.

Mabit, L., Bernard, C., 2007. Assessment of spatial distribution of fallout radionuclides through geostatistics concept. J. Environ. Radioact. 97, 206–219.

Moral, F.J., 2010. Comparison of different geostatistical approaches to map climate variables: application to precipitation. Int. J. Climatol. 30, 620–631.

Nanto, H., Takei, Y., Miyamoto, Y., 2011. Environmental background radiation monitoring utilizing passive solid sate dosimeters. In: Ekundayo, Ema O. (Ed.), Reference to a Chapter in an Edited Book: Environmental Monitoring, ISBN 978-953-307-724-6. Published: November 4, 2011.

Oliver, M.A., Webster, R., Lajaunie, C., Muir, K.R., Parkes, S.E., Cameron, A.H., Stevens, M.C.G., Mann, J.R., 1998. Binomial co-kriging for estimating and mapping the risk of childhood cancer. IMA J. Math. Appl. Med. 15 (3), 279–297.

O'Dea, J., Dowdall, M., 1999. Spatial analysis of natural radionuclides in peat overlying a lithological contact in Co. Donegal, Ireland. J. Environ. Radioact. 44, 107–117.

Quindós Poncela, L.S., Fernández, P.L., Gómez Arozamena, J., Sainz, C., Fernández, J.A., Suarez Mahou, E., Martin Matarranz, J.L., Cascón, M.C., 2004. Natural gamma radiation map (MARNA) and indoor radon levels in Spain. Environ. Int. 29, 1091–1096.

Rannou, A., Posny, F., Guezengar, J., Madelmont, C., 1984. Study of natural irradiation in dwelling places in France. Radiat. Prot. Dosim. 7, 317–320.

Rannou, A., Aubert, B., Scanff, P., 2006. Exposition de la population française aux rayonnements ionisants. Rapport IRSN, DRPH/SER, 2006-02, 11pp.

Ranogajec-Komor, M., Knežević, Z., Miljanić, S., Vekić, B., 2008. Characterisation of radiophotoluminescent dosimeters for environmental monitoring. Radiat. Meas. 43, 392–396.

Rivoirard, J., 2001. Which models for collocated cokriging. Math. Geol. 33 (2), 117–131.

Rivoirard, J., 2004. On some simplifications of cokriging neighbourhood. Math. Geol. 36 (8), 899–915.

Sanusi, M.S.M., Ramli, A.T., Gabdo, H.T., Garba, N.N., Heryanshah, A., Wagiran, H., Said, M.N., 2014. Isodose mapping of terrestrial gamma radiation dose rate of Selangor state, Kuala Lumpur and Putrajaya, Malaysia. J. Environ. Radioact. 135, 67–74.

Sundal, A.V., Strand, T., 2004. Indoor gamma radiation and radon concentrations in a Norwegian carbonatite area. J. Environ. Radioact. 77 (2), 175–189.

Szegvary, T., Conen, F., Stöhlker, U., Dubois, G., Bossew, P., de Vries, G., 2007. Mapping terrestrial gamma dose rate in Europe based on routine monitoring data. Radiat. Meas. 42, 1561–1572.

Report vol. I., 2008 UNSCEAR, 2008. Sources of Ionizing Radiation. United Nations Scientific Committee on the Effects of Atomic Radiation. In: UNSCEAR 2008 Report to the General Assembly, with Scientific Annexes, vol. I. Report to the General Assembly, Scientific Annexes A and B.